ARTICLE

# Efficiency Enhancement of Organic Photovoltaics by Introducing High-Mobility Curved Small-Molecule Semiconductors as Additives

Received 00th January 20xx,
Accepted 00th January 20xx

DOI: 10.1039/x0xx00000x

Shenghua Liu[a], Changqing Li[b], Xiaomin Xu[b], Peng You[a], Naixiang Wang[a], Jianfang Wang[c], Qian Miao[b,*], and Feng Yan[a,*]

Owing to their unique molecular geometry and packing modes in the solid state, curved organic semiconductor molecules such as hexabenzoperylenes and dibenzo[a,m]rubicene exhibit high hole mobilities of ~1 $cm^2$/Vs, which are much higher than the hole mobilities of the active layers in organic photovoltaics (OPVs). The efficiencies of OPVs based on the fullerene acceptor are relatively improved for over 20% by introducing the high-mobility curved p-type organic semiconductors in the active layers as additives for only a few weight percent. This can be attributed to the increased hole mobilities in the devices. In comparison, the significant efficiency enhancement cannot be observed when high-mobility planar molecules are introduced in the active layers. In view of the curved p-type semiconductor being more compatible with a fullerene acceptor in their molecular shape than a planar one, we consider that the intimate interaction between the curved molecule and the fullerene acceptor can enhance the exciton dissociation and hole transfer and thus boost the power conversion efficiencies of the devices.

## 1. Introduction

To meet the increasing demand for renewable energy, much attention has been paid to solar energy harvesting devices, particularly the photovoltaic cells. Solution-processed organic photovoltaics (OPVs) are one type of the most promising solar cells due to their low cost, light weight, and convenient fabrication processes.[1-6] Both non-fullerene and fullerene-based OPVs have been extensively studied in the past two decades and the device performance has been dramatically enhanced by various methods.[7-19] One bottleneck for the commercialization of OPVs is the relatively low power conversion efficiency (PCE) in comparison with their inorganic counterparts, which is mainly due to the low carrier mobilities and short exciton diffusion lengths in organic active layers.[20-23] An effective strategy is to introduce additional organic semiconductors into the active layers to tune the physical properties of the organic bulk heterojunctions.[24-30] For example, indene-$C_{60}$ bisadduct and poly-3-oxothieno[3,4-d]isothiazole-1,1-dioxide/benzodithiophene were added into the active layer of OPVs based on polythieno[3,4-b]-thiophene/benzodithiophene/[6,6]-phenyl$C_{71}$-butyric acid methyl ester (PTB7/$PC_{71}$BM) and dramatically enhanced the PCEs of the devices due to the improved charge separation and transportation as well as the enhanced light absorption in a broader wavelength region.[28, 29] The drawback of low carrier mobilities in OPVs was alleviated by introducing high-mobility conjugated polymers including alkyldiketopyrrolopyrrole-dithienylthieno[3,2-b]thiophene (DPP-DTT) and poly[2,5-bis(alkyl)pyrrolo[3,4-c]pyrrole-1,4(2H,5H)-dione-alt-5,5'-di(thiophene-2-yl)-2,2'-(E)-2-(2-(thiophen-2-yl)vinyl) thiophene] (PDVT-10) as additives in the devices and the device PCEs were substantially increased due to increased hole mobilities in the devices,[30] indicating that the addition of high-mobility organic semiconductors in OPVs is an effective approach for improving the device performance.

Various types of high-mobility organic semiconductors have been successfully synthesized specifically for the applications in organic field-effect transistors (OFETs) in recent years. For example, DPP-based conjugated polymer semiconductors have a wide range of mobilities from 0.1 to ~10 $cm^2V^{-1}s^{-1}$.[31] Poly[4-(4,4-dihexadecyl-4H-cyclopenta-[1,2-b:5,4-b']dithiophen-2-yl)-alt-[1,2,5]thiadiazolo[3,4-c]pyridine] (PCDTPT) shows a hole mobility higher than 10 $cm^2V^{-1}s^{-1}$.[32] Some small molecules, such as pentacene, rubrene and their derivatives, have demonstrated carrier mobilities much higher than 1 $cm^2V^{-1}s^{-1}$.[33-36] Besides, organic semiconductors based on nonplanar π-backbones exhibit hole mobilities of up to 1.0 $cm^2V^{-1}s^{-1}$ as a result of unconventional molecular packing with sufficient π-π stacking in the solid state. For example, the OFETs of hexabenzoperylene (HBP in Figure 1a) and dibenzo[a,m]rubicene (DBR in Figure 1a) were reported to exhibit hole mobilities as high as 0.82 $cm^2V^{-1}s^{-1}$ [37] and 1.0 $cm^2V^{-1}s^{-1}$, [38] respectively. These organic semiconductors have shown much higher carrier mobilities than the organic materials used in OPVs. Thus, it is convenient to utilize the high-mobility organic semiconductors in OPVs as additives to improve their PCEs.

[a] Department of Applied Physics, The Hong Kong Polytechnic University, Hong Kong, China. E-mail: apafyan@polyu.edu.hk
[b] Department of Chemistry, The Chinese University of Hong Kong, Shatin, Hong Kong, China. E-mail: miaoqian@cuhk.edu.hk
[c] Department of Physics, The Chinese University of Hong Kong, Shatin, Hong Kong, China.

Electronic Supplementary Information (ESI) available: [details of any supplementary information available should be included here]. See DOI: 10.1039/x0xx00000x

In this work, we introduced high-mobility small molecules, including HBP and DBR, into the active layers of OPVs. It is interesting to find that the addition of 2.5 wt.% HBP can lead to a dramatic increase in the PCE of PTB7/$PC_{71}BM$-based OPVs from 7.80% to 9.54%. Similarly, for another type of OPVs based on poly[4,8-bis(5-(2-ethylhexyl)thiophen-2-yl)-benzo[1,2-b;4,5-b']dithiophene-2,6-diyl-alt-(4-(2-ethylhexyl)-3-fluorothieno[3,4-b]thiophene-)-2-carboxylate-2-6-diyl)](PBDTTT-EFT) and $PC_{71}BM$, the addition of 2.5 wt.% DBR can improve the average PCE from 9.09% to 10.43%, and the efficiency could be further enhanced to over 11% by incorporating plasmonic Au@Ag core-shell nanocuboids (NCs) in the devices. We find that the carrier mobility of the additive is a critical issue for the PCE enhancement. The performance enhancement is attributed to the increase of hole mobility in the active layers of OPVs. In addition, we studied the influence of the molecular shape of the additve on the device performance. When a high-mobility planar molecule TIPs-pentacene was added into the OPVs, little enhancement in the device efficiency was observed. We also find that the organic semiconductor additive with a curved surface can have a stronger interaction with $PC_{71}BM$. These results imply that high-mobility curved molecules can have more efficient charge transfer with $PC_{71}BM$ in the active layers of OPVs. This work provides a guideline for the design of small-molecule additives to improve the efficiency of OPVs.

## 2. Results and Discussion

OPVs based on PTB7/$PC_{71}BM$ and PBDTTT-EFT/$PC_{71}BM$ were fabricated with the conventional device architecture shown in **Figure 1a**. Poly(3,4-ethylenedioxythiophene):polystyrene sulphonic acid (PEDOT:PSS) and Ca were used as the hole transport layer (HTL) and electron transport layer (ETL) of the device, respectively. Three organic semiconductors were used as additives in the active layers of the OPVs, including nonplanar molecules HBP, DBR and planar molecule TIPs-Pentacene. **Figure 1b** shows the configuration of the three molecules adjacent to a $PC_{71}BM$ molecule. So the curved molecules (HBP and DBR) may have more intimate interactions with $PC_{71}BM$ than the planar molecule TIPs-Pentacene. **Figure 1c** shows the energy level alignment of the OPVs when the three additives are introduced in the active layers. All the energy levels of PTB7, $PC_{71}BM$ and additives, including HBP, DBR, TIPs-Pentacene chosen from literatures were determined by the cyclic voltammetry method.[30, 37-39] The lowest unoccupied molecular orbital (LUMO) levels of PTB7 and HBP are very close, which benefits the electron transport in the mixture of the two materials. More importantly, the cascaded highest occupied molecular orbital (HOMO) levels of PTB7, HBP and $PC_{71}BM$ are favorable for hole transfer from the active layer to the PEDOT:PSS HTL. Notably, DBR and TIPs-Pentacene can also form a cascade energy level alignment in the OPVs, which is favorable for charge transfer in the devices.

### 2.1 Effect of HBP in OPVs

The current density-voltage (*J-V*) characteristics of the PTB7/$PC_{71}BM$ -based OPVs with different percentages of HBP are presented in **Figure 2a**. Detailed photovoltaic parameters including open-circuit voltage ($V_{oc}$), short circuit current ($J_{sc}$), fill factor (FF), PCE and relative PCE enhancement are summarized in **Table S1** in the supplementary information. It can be found that the additions of HBP increase the device performance substantially, and 2.5 wt.% HBP addition leads to the best photovoltaic performance with $J_{sc}$ of 18.86 mA/cm$^2$, $V_{oc}$ of 0.746 V, FF of 67.8% and an average PCE of 9.54%. So the PCEs of the devices are relatively enhanced for over 20% at the optimum condition. However, further increase of the addition level of HBP to 5 wt.% inversely decreases the average PCE to 8.54%. The variation of the device photovoltaic performance with the addition of HBP can also be reflected in the external quantum efficiency (EQE) spectra in **Figure 2b**. Compared with the control device with the maximum EQE of 71.9%, the devices added with 1 wt.% and 2.5 wt.% HBP show improved EQE values in the whole characterized wavelength region with the maximum values of 80.1% and 85.4%, respectively. However, more addition of HBP (5.0 wt.%) into the active layer leads to the decrease of EQE, which is consistent with the *J-V* plots in **Figure 2a**.

Notably, HBP is a twisted small molecule and can be converted into a mixture of twisted and anti-folded isomers at a high temperature ($\geq$ 70 °C).[37, 40] The twisted & anti isomer was actually found to have a much lower mobility in OFETs, which is unfavorable for carrier transfer in OPVs. To test this effect, we heated the blend precursors with HBP additive at 70 °C for over 1 hour and then cooled it to room temperature for spin coating. OPVs fabricated from the heated solution were characterized at the same conditions. It is notable that the efficiency of the devices degraded rapidly as demonstrated in the *J-V* curves in **Figure 2c**. With increased additions of twisted & anti HBP from 1 wt.% to 5.0 wt.% in active layers, the average PCEs of the devices decrease significantly from 7.3% to 6.24%. Detailed photovoltaic parameters can be found in **Table S2** in the supplementary information. **Figure 2d** shows the PCEs of the devices with the addition of HBP at two different conditions. It can be observed that the performance of OPVs was dramatically enhanced by HBP when the devices were prepared at room temperature while the PCE of the OPVs decreased obviously when twisted & anti HBP was used. The negative effect of the twisted & anti HBP in the devices can be attributed to the low carrier mobilities of the treated HBP.

To better understand the effect of HBP on the OPVs, hole-transfer devices with the device structure of ITO/PEDOT:PSS/blend layer/Au and electron-transfer devices with the structure of ITO/ZnO/blend layer/Al were prepared (See supplementary information). Electron and hole currents versus bias voltage were measured in the devices with different percentages of HBP (See supplementary information, **Figure S1**). The plots can be well fitted by the space charge limited currents (SCLCs) equation. The calculated hole and electron mobilities as a function of the addition amount of HBP were summarized in **Figure 2e**. We can clearly find that the hole mobility increases gradually with the increase of the HBP amount while the electron mobility inversely decreases. Notably, the hole and electron mobilities become more balanced when 2.5 wt.% HBP is added, which is favorable for charge transfer in the OPVs. However, the devices fabricated from the heated blend solutions without any change of the other conditions demonstrate completely different variations of the electron and hole currents (See supplementary information, **Figure S1**). The calculated hole and electron mobilities in **Figure 2f** further illustrate that the carrier mobilities in

 

PTB7+HBP/$PC_{71}BM$ blends are hardly influenced by twisted & anti HBP owing to its low hole mobility.

The effect of HBP additive was also tested in the OPVs based on PBDTTT-EFT/$PC_{71}BM$ that were expected to have higher PCEs due to the broader light absorption region of PBDTTT-EFT. **Figure 3a and 3b** show the *J-V* and EQE curves of the OPVs with different addition amounts of HBP. The detailed photovoltaic parameters are presented in the supplementary information (**Table S3**). An obvious PCE enhancement induced by HBP in the devices can be observed, as shown in **Figure 3c**. The average PCE of the devices increases when 1.0 wt.% HBP is added, but then decreases when the addition level is further increased. The addition of HBP led to the maximum average PCE of 9.91±0.10% with a relative enhancement of 9.75% over the control devices.

**2.2 Effect of DBR in OPVs**

DBR is another nonplanar organic semiconductor with a hole mobility up to 1.0 $cm^2 V^{-1}s^{-1}$.[38] We fabricated the OPVs based on PTB7+DBR/$PC_{71}BM$ at the identical conditions as mentioned above. The *J-V* and EQE characteristics of the OPVs incorporated with different concentrations of DBR in their active layers are shown in **Figure 4a-c**. Detailed photovoltaics parameters of the devices are presented in **Table S4** in the supplementary information. The control devices without the addition of DBR show an average PCE of 7.72%, while the devices added with 2.5 wt.% DBR present the highest average PCE of 8.63%, demonstrating a relative enhancement of 11.8%. The results are consistent with the EQE enhancement in the wavelength range of 300-400 nm and 550-700 nm. However, the performance enhancement induced by DBR is lower than that resulted from HBP.

Next, the effect of DBR was tested in OPVs based on PBDTTT-EFT/$PC_{71}BM$. **Figure 4d and 4e** show the *J-V* and EQE curves for the devices added with DBR for different percentages, demonstrating more significant improvement in the device performance than the effect of HBP. The photovoltaic parameters of the devices are summarized in **Table S5** in the supplementary information. The PBDTTT-EFT/$PC_{71}BM$ control devices without the additive give an average $V_{oc}$ of 0.769 V, $J_{sc}$ of 17.64 mA/$cm^2$, FF of 67.0% and an average PCE of 9.09%. For the devices added with 1 wt.% DBR, the PCE is improved to 9.70% in average. Then the average PCE is further improved to 10.43% when the addition amount of DBR is increased to 2.5 wt.% and the champion device shows the PCE of 10.62%. However, more addition of DBR to 5 wt.% cannot enhance device performance anymore, giving an average device PCE of only 9.33%. The EQE characterization of the OPVs presented in **Figure 4e** is also consistent with the variation of $J_{sc}$. The control device without the additive exhibits the maximum EQE of 75.47%, while the devices with the DBR addition levels of 1.0 and 2.5 wt.% show the maximum EQE of 82.22 and 87.04%, respectively. Further addition of DBR (5.0 wt.%) decreases the EQE values in the wavelength range between 500 nm and 650 nm. The PCEs of the devices as a function of DBR level are summarized in **Figure 4f.** Compared with HBP, DBR can induce a higher PCE enhancement (relatively 14.7%) in OPVs based on PBDTTT-EFT/$PC_{71}BM$. Additionally, the effect of DBR has also been tested in the traditional OPVs based on poly(3-hexylthiophene) (P3HT)/$PC_{71}BM$ and the novel nonfullerene system based on PBDB-T-SF/IT-4F.[41, 42] As shown in **Figure S2** in the supplementary information, the *J-V* and EQE curves indicate that the addition of 2.5 wt.% DBR can improve the PCE of the OPVs based on P3HT/$PC_{71}BM$ from 4.01% (control device) to 4.64% at the optimum condition. More detailed device performances can be found in **Table S9** in the supplementary information. However, when DBR was added into the PBDB-T-SF/IT-4F based OPVs, the results showed a significantly different effect. As depicted in figure S3 and table S10 in the supplementary information, the efficiency of the devices monotonously decreases with the increase of the addition level of DBR. When 5 wt.% DBR was added into the PBDB-T-SF/IT-4F active layers, the average PCE of the OPVs decreased from 10.25% (control device) to 8.79%. The different effects of DBR on the two systems based on fullerene and nonfullerene acceptors indicate that the curved molecule DBR has an interaction with orbicular fullerene acceptor, which can lead to the improvement of the device performance. However, when DBR was added into the nonfullerene devices based on planar active layer materials of PBDB-T-SF/IT-4F, no positive effect was observed.

To further improve the device performance of the OPVs based on PBDTTT-EFT+DBR/$PC_{71}BM$, Au@Ag core-shell NCs were incorporated into the PEDOT:PSS HTL to enhance the light absorption of the active layer via the light scattering effect and the near-field enhancement of the NCs. The structure of the plasmonic device is shown in **Figure 5a**. The sizes of the Au@Ag NCs were optimized to be 20nm for the Ag shell thickness and 20nm/60 nm for the diameter/length of the Au core. The Au@Ag NCs were synthesized by the method reported before to realize a broad band enhancement of light absorption in the visible region.[22, 43] **Figure 5b** shows the *J-V* curves of the OPVs with different addition levels of Au@Ag NCs. Average photovoltaic parameters over 3 identical devices are summarized in the supplementary information in **Table S6**. Without the incorporation of NCs, the control devices based on PBDTTT-EFT+DBR/$PC_{71}BM$ give an average $V_{oc}$, $J_{sc}$, and FF of 0.792V, 18.93 mA/$cm^2$, and 68.5%, respectively, leading to an average PCE of 10.27%. After adding Au@Ag NCs in PEDOT:PSS HTLs, the performance of the OPVs exhibits an obvious improvement. Specifically, with 1 vol.% and 5 vol.% introduction of NCs, the $V_{oc}$ of the devices remains unchanged, while $J_{sc}$ is increased to 19.32 and 20.29 mA/$cm^2$ and FF is enhanced to 70.0% and 70.7%, respectively. As a result, the corresponding average PCEs are improved to 10.76% and 11.42%, as shown in **Figure 5c**. Notably, the PCE of our devices is close to the record of fullerene-based OPVs reported recently.[44]

EQEs of the OPVs were measured to better elucidate the improved $J_{sc}$. As shown in **Figure 5d**, EQEs of the devices are improved in the whole characterized region by the NCs. The device with NCs (5.0 vol% solution) incorporated in the PEDOT:PSS layer shows the maximum EQE value of 86.35% in comparison with the control devices with 78.96%, and as expected, it is better than the device containing 1.0 vol% NCs with the maximum EQE of 80.93%. The cooperative plasmonic effect of the NCs and the enhancement of the hole mobility with addition of DBR, both improve the performance of the OPVs. The dual effects increase the average PCE from 9.09% to over 11%. A pronounced relative PCE enhancement up to 25.63% can be

observed, which is mainly due to the remarkable increase of the $J_{sc}$ of the devices.

### 2.3 Effect of TIPs-Pentacene in OPVs

TIPs-Pentacene is a high-mobility small-molecule p-type semiconductor popularly used in OFETs,[36] but, unlike HBP and DBR, has a planar π-backbone. TIPs-Pentacene was introduced into the OPVs based on PTB7/$PC_{71}BM$ and PBDTTT-EFT/$PC_{71}BM$ and prepared at the same processing conditions mentioned above. The *J-V* curves and photovoltaic parameters of the two types of devices are shown in **Figure 6a** and **6b**, respectively (Supplementary information, **Table S7** and **Table S8**). For PTB7/$PC_{71}BM$-based OPVs, the maximum efficiency of 8.6% was achieved when 1 wt.% TIPs-Pentacene was added into the active layer of the device, leading to around 7.9% relative enhancement of PCE in comparison with the control device. However, further increase of the addition level cannot enhance the device performance (**Figure 6c**). For the OPVs based on PBDTTT-EFT/$PC_{71}BM$, the device PCE is enhanced a little bit by TIPs-Pentacene. As shown in **Figure 6d**, the PCE is enhanced from 8.82% to 9.06% with the maximum relative enhancement of 2.7% at the addition level of 1.0 wt.%. Therefore, the enhancement induced by TIPs-pentacene in the OPVs is much lower than those induced by HBP and DBR.

Considering that the light absorption of the blend film can be changed by the additives, we have characterized the UV-visible absorption spectra of the three types of additives in dichloromethane solution with the same concentration of $5\times10^{-6}$ M and the blended active layer thin films based on PTB7/$PC_{71}BM$ with and without the additives (2.5 wt.% relatively to PTB7). As depicted in figure S4 in the supplementary information, the additions of 2.5 wt.% HBP, DBR, or TIPs-pentacene can enhance the light absorption of the blend films in the wavelength range of 300-600 nm, which is probably due to the change of the film thickness and the crystallinity of the doner and acceptor phases. Obviously, the change of absorption spectra cannot be attributed to the light absorption of the additives because the additives only demonstrate several absorption peaks in narrow wavelength regions. Although the enhanced light absorption of the blend films can be a possible reason for the incresed $J_{sc}$ of the OPVs, it is not the dominant factor for the efficiency enhancement because TIPs-pentacene can increase the light absorption with the highest magnitude while the resultant $J_{sc}$ enhancement of the devices shows the minimum value in the three additives. The above experimental results indicate that small-molecule high-mobility organic semiconductors can enhance the PCEs of OPVs based on different active layer materials. When the carrier mobility of the added small molecules (e.g. HBP and twisted & anti isomer) is decreased, the PCE enhancement of the OPVs disappears. Another interesting finding here is that the molecular structure of the small molecules can influence the PCE enhancement in OPVs for different levels. Although TIPs-Pentacene has a higher carrier mobility than HBP and DBR, the PCE enhancement induced by planar TIPs-Pentacene is much lower than those induced by curved HBP and DBR.

### 2.4 Interactions between additives and $PC_{71}BM$

We consider that the interaction between the small-molecule additive and $PC_{71}BM$ can be a dominant factor for the PCE enhancement. For curved molecules, a more intimate interaction may exist between the additive and $PC_{71}BM$, as depicted in **Figure 1b**, which can enhance charge transfer between them. To confirm this effect, we characterized Fourier-transform infrared spectroscopy (FTIR) of PTB7/$PC_{71}BM$ blend films with different additives, including HBP, DBR and TIPs-Pentacene, as shown in **Figure 7a** and **7b**. It is notable that the absorption peak at 1450 $cm^{-1}$ for $PC_{71}BM$ is broadened by HBP and DBR while TIPs-Pentacene has little effect on the peak width.[45] These results suggest that $PC_{71}BM$ has stronger interactions with HBP and DBR than with TIPs-Pentacene presumably because the curved shape of HBP and DBR is complementary to the ellipsoid shape of $C_{70}$. It is notable that charge transfer rate from one molecule to another is related to the electron coud everlap. So the stronger interactions are favorable for charge transfer between $PC_{71}BM$ and the additive.[46] However, the curved molecules can not show an obvious advantage on charge transfer when they are placed together with conjugated polymer donors.

The surface morphologies of the blend films based on PTB7/ $PC_{71}BM$ before and after the addition of 2.5 wt.% HBP/DBR have also been characterized by AFM. As depicted in figure S5 in the supplementary information, no obvious change can be observed on the surface morphology of the thin films. Only the surface roughness of the thin films increased gradually from 0.95 nm of the pristine PTB7/$PC_{71}BM$ film to 1.08 and 1.25 nm with addition of HBP and DBR, respectively. The additives of HBP/DBR do not change the structures of the blend films, which guarantees the efficient charge transfer in the active layer of the devices.

The organic blend films with different additives were characterized under Grazing Incidence X-Ray Diffraction (GIXD, Regaku 9KW SmartLAB). The out-of-plane diffraction peaks of different films are shown in **Figure 7c** and **7d**. Each peak for pure $PC_{71}BM$ and PTB7 films can be fitted very well with a Lorentz function (see supplementary information).[30] The peak for pure PTB7 at q=1.60 $Å^{-1}$ corresponds to the lattice plane (010).[29] The broad peaks (I, II) of the pure $PC_{71}BM$ film at q=0.70 and 1.32 $Å^{-1}$ can be attributed to the combination of several peaks corresponding to different lattice planes.[47] It is reasonable to observe a broader diffraction peak in a PTB7/$PC_{71}BM$ blend film, which is the combination of the two peaks at q=1.32 $Å^{-1}$ and 1.60 $Å^{-1}$ originated from $PC_{71}BM$ and PTB7, respectively. By doing least square fitting, we can extract the width of the diffraction peak of $PC_{71}BM$ at q=1.32 $Å^{-1}$. As shown in **Figure 7d**, the width is increased due to the addition of HBP and DBR, while TIPs-Pentacene in the blend film cannot induce a detectable change of the peak width. The broadening of the diffraction peak can be attributed to the decrease of the crystallinity of $PC_{71}BM$ in the blend films. The lower crystallinity of $PC_{71}BM$ is presumably due to a strong interaction between $PC_{71}BM$ and HBP (DBR) in the organic films as a result of complementary shapes of fullerene and HBP. This result also explains the decrease of electron mobility with the addition of HBP in the PTB7/$PC_{71}BM$ blend film presented in **Figure 2e**. An illustration of the working mechanism is proposed in **Figure 7e**. The FTIR and XRD results suggest that $PC_{71}BM$ has a stronger interaction with curved HBP and DBR than with TIPs-Pentacene. Additionally, the molecular ordering of PTB7 has no obvious change with the introduction of additives, which demonstrates that the curved small molecules HBP

 

and DBR are mainly located at the interface between PTB7 and $PC_{71}BM$. Not only the complementary shapes of fullerene and curved additives but also the high hole mobilities of HBP and DBR can enhance charge transfer in the donor/acceptor heterojunctions, which eventually results in the efficiency improvements of the OPVs with the appropriate additions of the curved molecules.

## 3. Experimental Section

**Materials**: The materials of polythieno[3,4-b]-thiophene-benzodithiophene (PTB7), [6,6]-phenyl $C_{71}$-butyric acid methylester ($PC_{71}BM$) and poly[4,8-bis(5-(2-ethylhexyl)thiophen-2-yl)-benzo[1,2-b;4,5-b']dithiophene-2,6-diyl-alt-(4-(2-ethylhexyl)-3-fluorothieno[3,4-b]thiophene-)-2-carboxylate-2-6-diyl)] (PBDTTT-EFT) were purchased from 1-Materials Incorporation. Poly(3,4-ethylenedioxythiophene):polystyrene sulphonic acid (PEDOT:PSS) (CLEVIOS™ PH 500) was purchased from Heraeus, Germany. The high-mobility small molecules HBP, DBR, and TIPs-Pentacene were synthesized by the method reported previously.[37, 38]

**Fabrication of devices**: The device structure of the solution processed OPV is shown in **Figure 1a**. A high mobility small molecule (HBP, DBR and TIPs-pentacene) was added into the active layer based on PTB7/$PC_{71}BM$ (1:1.5 weight ratio) in the mixed solvent of chlorobenzene (CB) and 1,8-diiodoctane (DIO) (97:3 volume ratio). The PTB7/$PC_{71}BM$-based OPVs with various addition levels of HBP (HBP weight percentages relative to PTB7 are 1%, 2.5% and 5%) were fabricated at the identical conditions. A ~40 nm PEDOT:PSS layer was spin-cast on the patterned ITO/glass subsrates and then annealed at 150℃ for 30 min. After that, the active layer was spin-cast on the PEDOT:PSS layer from the PTB7(+HBP, DBR, and TIPs-Pentacene)/$PC_{71}BM$ precursors at 1500rpm for 1 min in a glovebox. Before electrode deposition, methanol was spin-coated onto the active layer at 2500 rpm. Then, a Ca layer with thickness of 20 nm and a 100 nm Al electrode were sequentially deposited on the active layer by thermal evaporation. The area of the active layer was 6.0 $mm^2$.

The OPVs based on PBDTTT-EFT/$PC_{71}BM$ with the addition of HBP, DBR, or TIPs-Pentacene were also prepared at exactly the same fabrication condition as PTB7/$PC_{71}BM$-based devices. The addition percentages of the small molecules relative to PBDTTT-EFT in the experiments are 1.0, 2.5, and 5.0 wt.%, respectively. The P3HT/$PC_{71}BM$- and PBDB-T-SF/IT-4F-based OPV devices with and without DBR (1.0, 2.5, and 5.0 wt.%) were fabricated at the conditions according to the previous reports.[41, 42] All of the OPV devices were encapsulated in the glovebox, then characterized in air and at least 6 devices were prepared for each condition.

Hole-only and electron-only devices were fabricated for measuring hole and electron mobilities in PTB7+HBP/$PC_{71}BM$ blend films. Hole-only devices with the structure of ITO/PEDOT:PSS/blend layer/Au were prepared by spin coating the PEDOT:PSS and PTB7+HBP/$PC_{71}BM$ films subsequently on ITO glass substrates in the glovebox, followed by the thermal deposition of an Au top electrode through a shadow mask. The average thickness of the PTB7+HBP/$PC_{71}BM$ films was characterized to be 250 nm under atomic force microscopy (AFM, Digital Instruments). Electron-only devices with the structure of ITO/ZnO/blend layer/Al were prepared. ZnO precursor solution (0.5M zinc acetate dehydrate in 2-methoxyethanol) was spin coated on ITO substrates at 3000rpm for 30s, followed by thermal annealing on a hotplate at 200 °C for 30 min in dry air. Then PTB7+HBP/$PC_{71}BM$ films were coated on the ZnO layers. Finally, Al top electrodes were deposited by thermal evaporation through a shadow mask.

**Characterization**: The current density-voltage (*J-V*) characteristics of the OPVs were measured by using a Keithley 2400 source meter under illumination of 100 $mW/cm^2$ (Newport 91160, 300 W, solar simulator equipped with an AM 1.5 filter). The light intensity was calibrated with a standard silicon solar cell. EQE spectra of the OSCs were measured with a standard system equipped with a xenon lamp (Oriel 66902, 300W), a monochromator (Newport 66902), a Si detector (Oriel 76175_71580), and a dual channel power meter (Newport 2931_C). FTIR spectra of organic films were measured by using Bruker VERTEX 70 FT-IR spectrometer.

The space charge limited currents (SCLCs) of the hole-only devices and electron-only devices were characterized by the semiconductor parameter analyzer (Agilent 4156C) in the glovebox. The current density as a function of bias voltage was fitted (least-square fitting) with the Murgatroyd equation:[30]

$$J = \frac{9}{8}\varepsilon_r\varepsilon_0\mu e^{0.89\beta\sqrt{(V-V_b)/d}}\frac{V^2}{d^3} \quad (1)$$

where $V$ is the applied voltage, $\varepsilon_r$ is the relative permittivity of the organic blend (taken as 3.5), $\varepsilon_0$ is the permittivity of free space, $\mu$ is the carrier mobility. $\mu$, $\beta$ and $V_b$ are fitting parameters.

Orgnanic blend films coated on $SiO_2$/Si substrates were characterized with Grazing Incidence X-Ray Diffraction (GIXD, Regaku 9KW SmartLAB). Each peak was fitted with the Lorentz function:[30]

$$I = I_b + \frac{2A}{\pi}\frac{w}{4(q-q_p)^2+w^2} \quad (2)$$

where $I$ is the intensity, $I_b$ is the background intensity, $A$ is the peak area, $w$ is the half-width and $q_p$ is the peak position.

ARTICLE

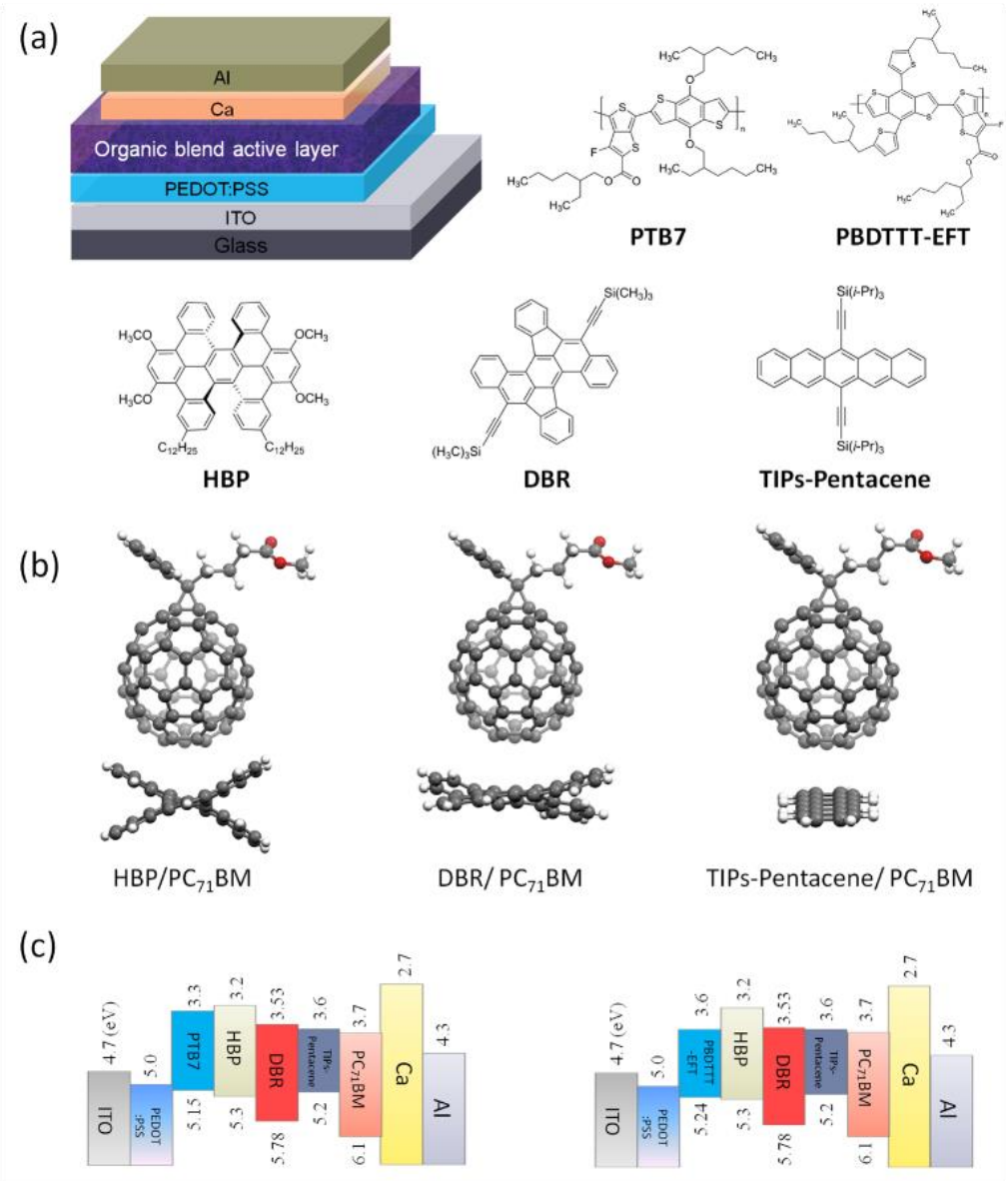


**Figure 1.** (a) Device architecture of the OPVs and the molecular structures of the p-type polymers used in the devices, including PTB7 and PBDTTT-EFT, (b) Intermolecular correlation between the backbone of HBP, DBR, TIPs-Pentacene and $PC_{71}BM$ with 3D molecular structures. (c) Energy level alignments of OPVs based on PTB7/ $PC_{71}BM$ (left) and PBDTTT-EFT/$PC_{71}BM$ (right) with the introduction of different additives.

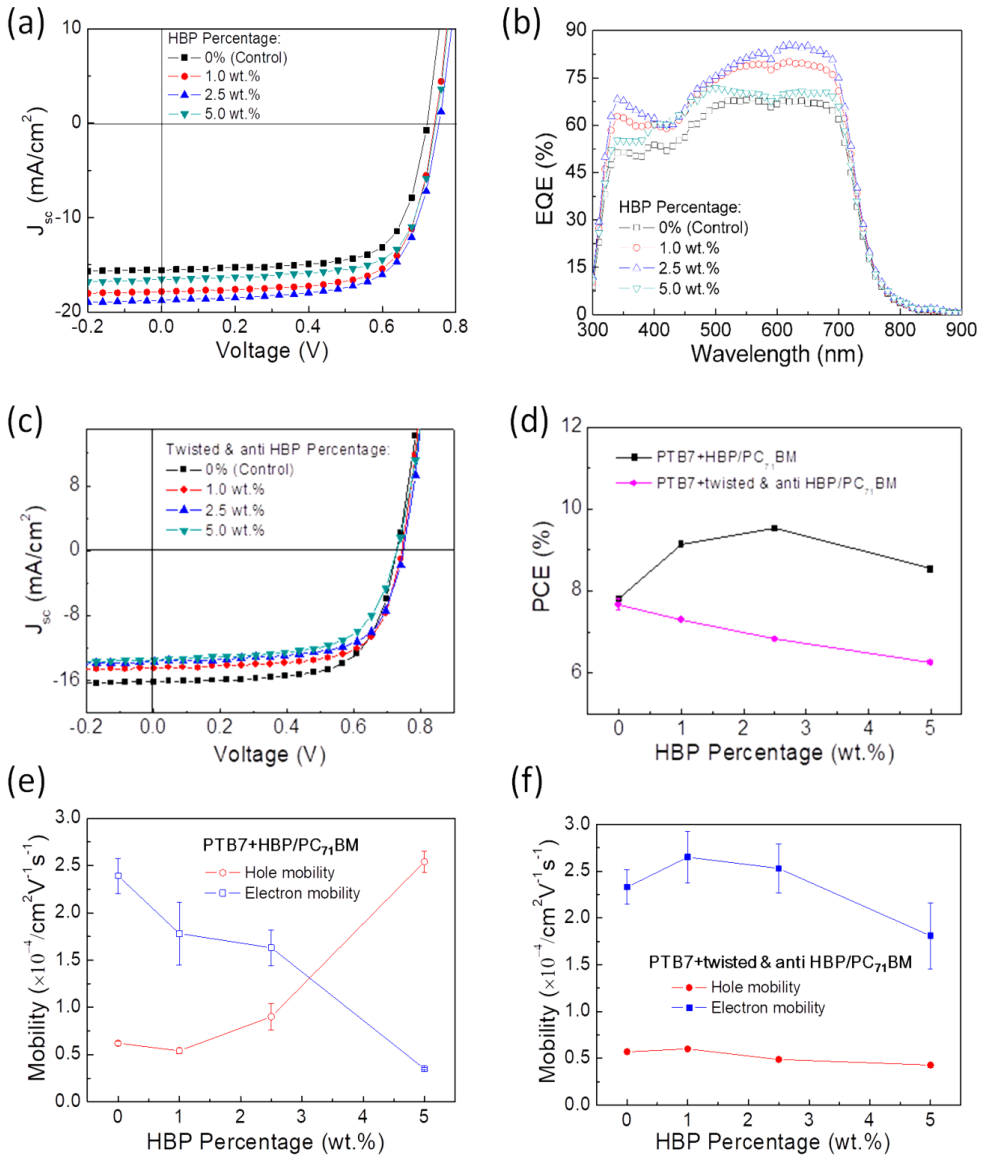


**Figure 2.** (a) *J-V* and (b) EQE curves of the best OPV based on PTB7/$PC_{71}BM$ with HBP as additive; (c) *J-V* curves of the best OPV based on PTB7/$PC_{71}BM$ with low-mobility twisted & anti HBP as additive; (d) Average PCEs of the OPVs based on PTB7+HBP/$PC_{71}BM$ with the additions of high-mobility HBP and low-mobility twisted & anti HBP; (e) Electron and hole mobilities calculated from the SCLCs in the devices with high-mobility HBP; (f) Electron and hole mobilities calculated from the SCLCs in the devices with low-mobility twisted & anti HBP.

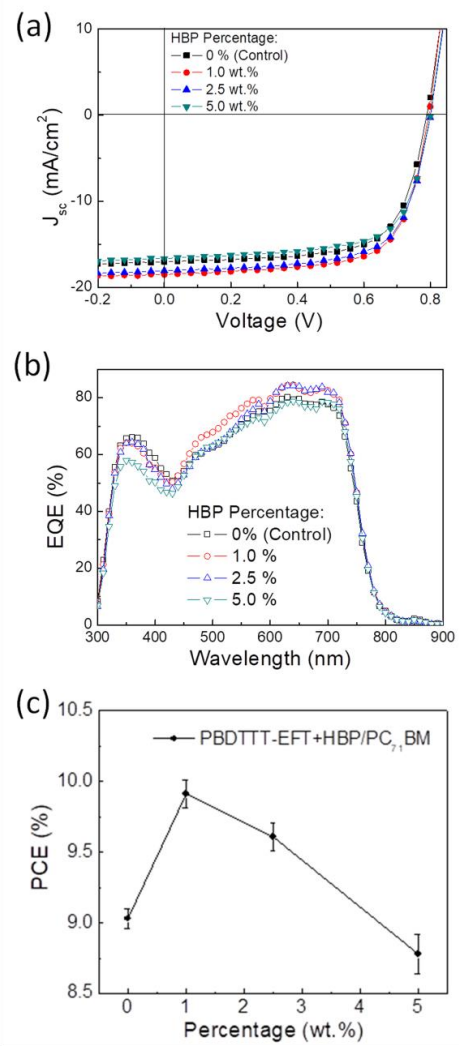


**Figure 3.** (a) *J-V* and (b) EQE curves of the OPV based on PBDTTT-EFT/$PC_{71}BM$ with HBP as additive, (c) The variation of the average PCEs of the OPVs with different addition level of HBP.

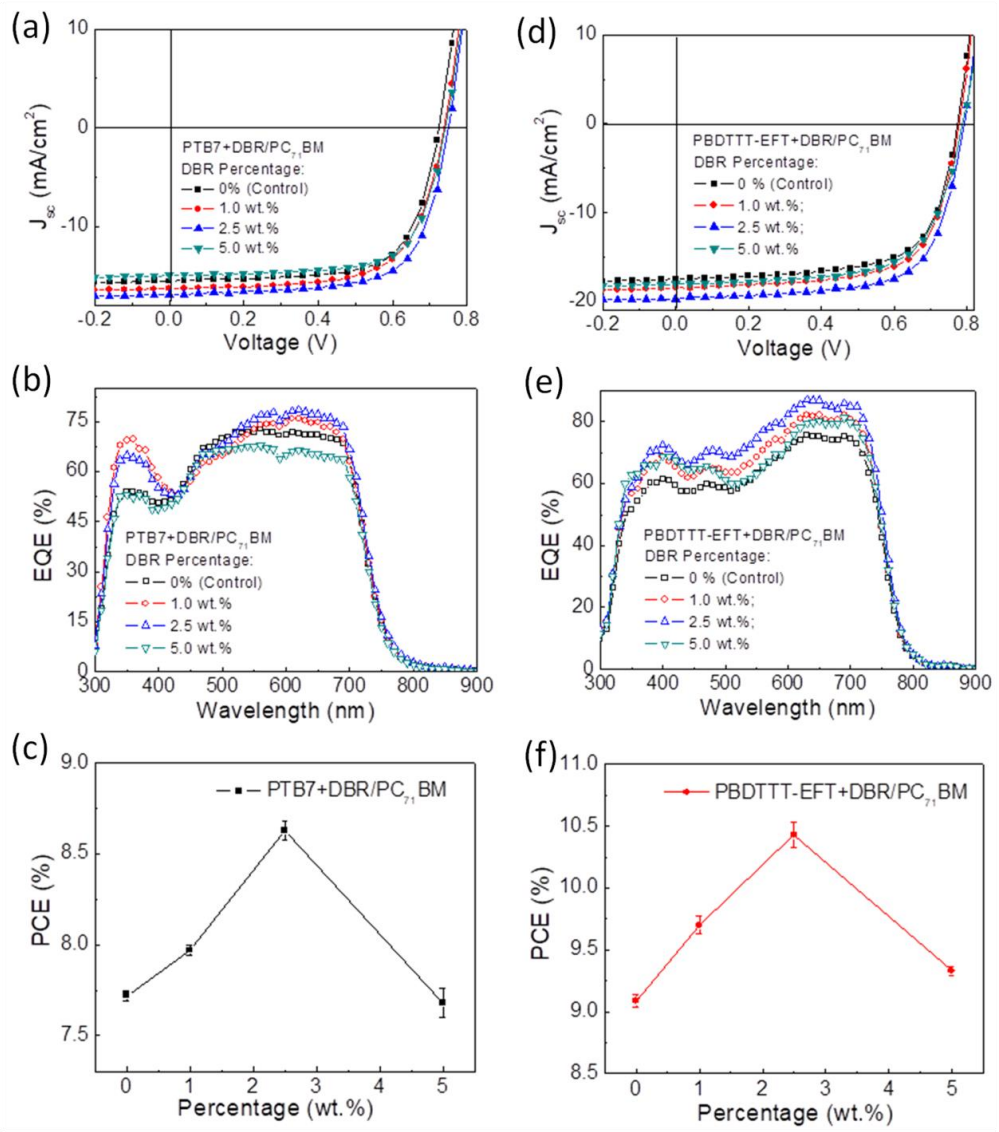


**Figure 4.** (a) *J-V* and (b) EQE curves of the OPVs based on PTB7/$PC_{71}BM$ with DBR as additive; (c) The variation of the average PCEs of the OPVs with different addition amount of DBR; (d) *J-V* and (e) EQE curves of the OPV based on PBDTTT-EFT/$PC_{71}BM$ with DBR as additive; (f) The variation of the average PCEs of the devices with different addition amount of DBR.

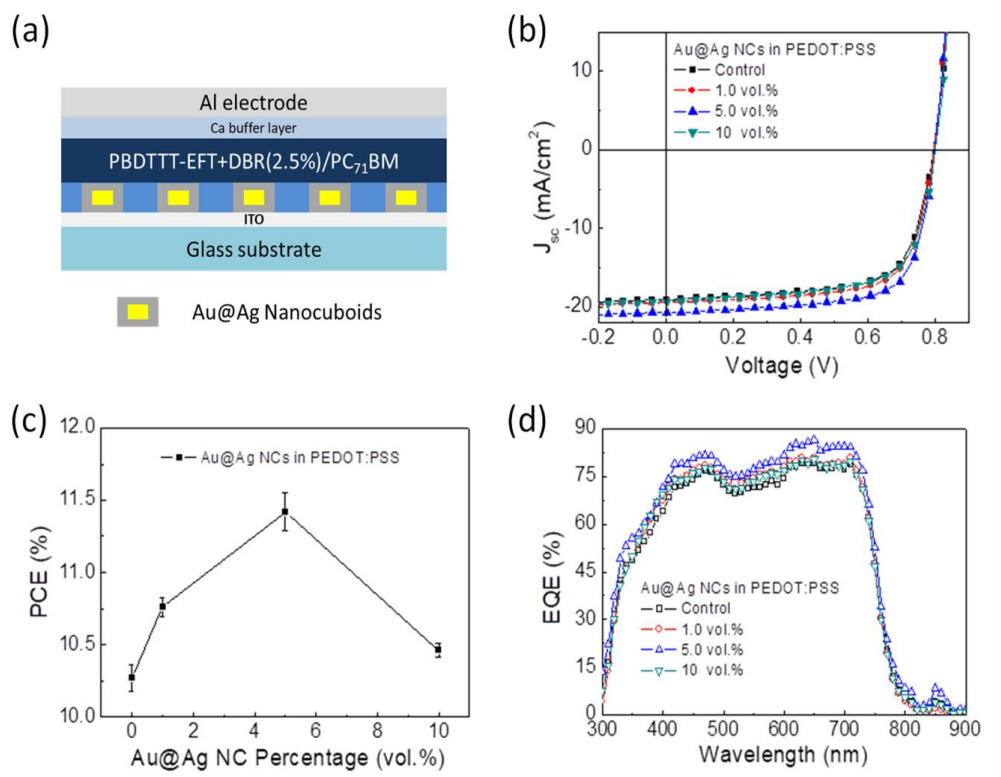


**Figure 5.** (a) The device structure of the plasmonic OPVs based on PBDTTT-EFT+DBR/$PC_{71}BM$. (b) *J-V* curves (c) average PCE and (d) EQE spectra of the OPVs based on PBDTTT-EFT+DBR/$PC_{71}BM$ incorporated with different addition levels (solution volume percentage) of Au@Ag NCs in PEDOT:PSS.

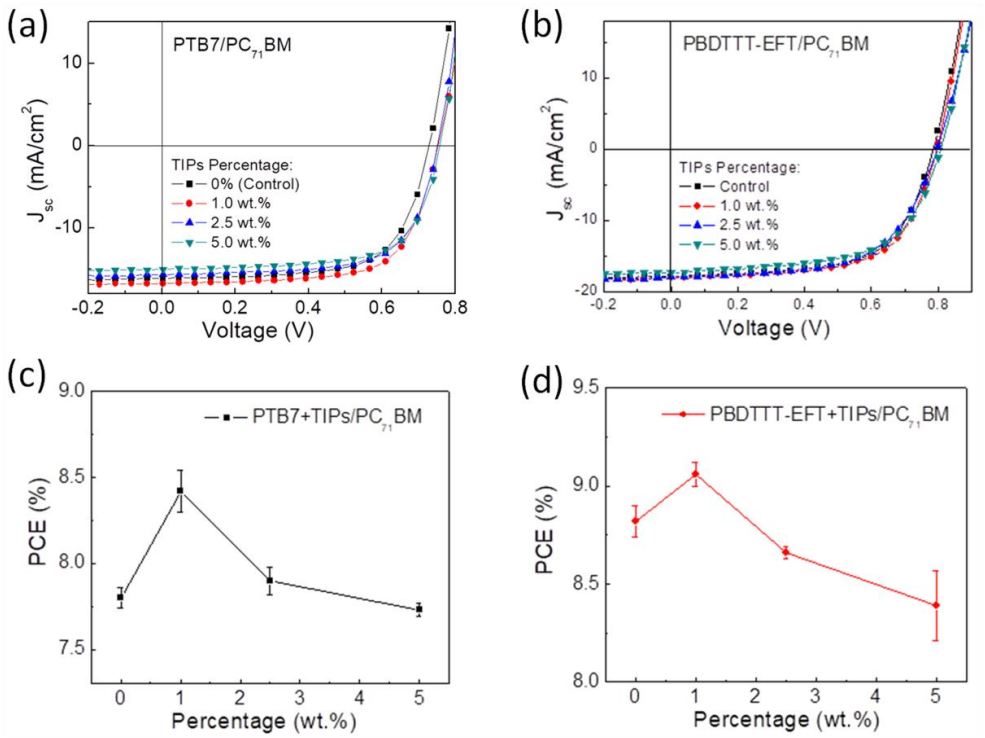


**Figure 6**. *J-V* curves of the OPVs based on (a) PTB7/$PC_{71}BM$, (b) PBDTTT-EFT/$PC_{71}BM$ with TIPs-Pentacene as additive. (c) The variation of the average PCEs of the OPVs based on (c) PTB7/$PC_{71}BM$, (d) PBDTTT-EFT/$PC_{71}BM$ with different addition amount of TIPs-Pentacene.

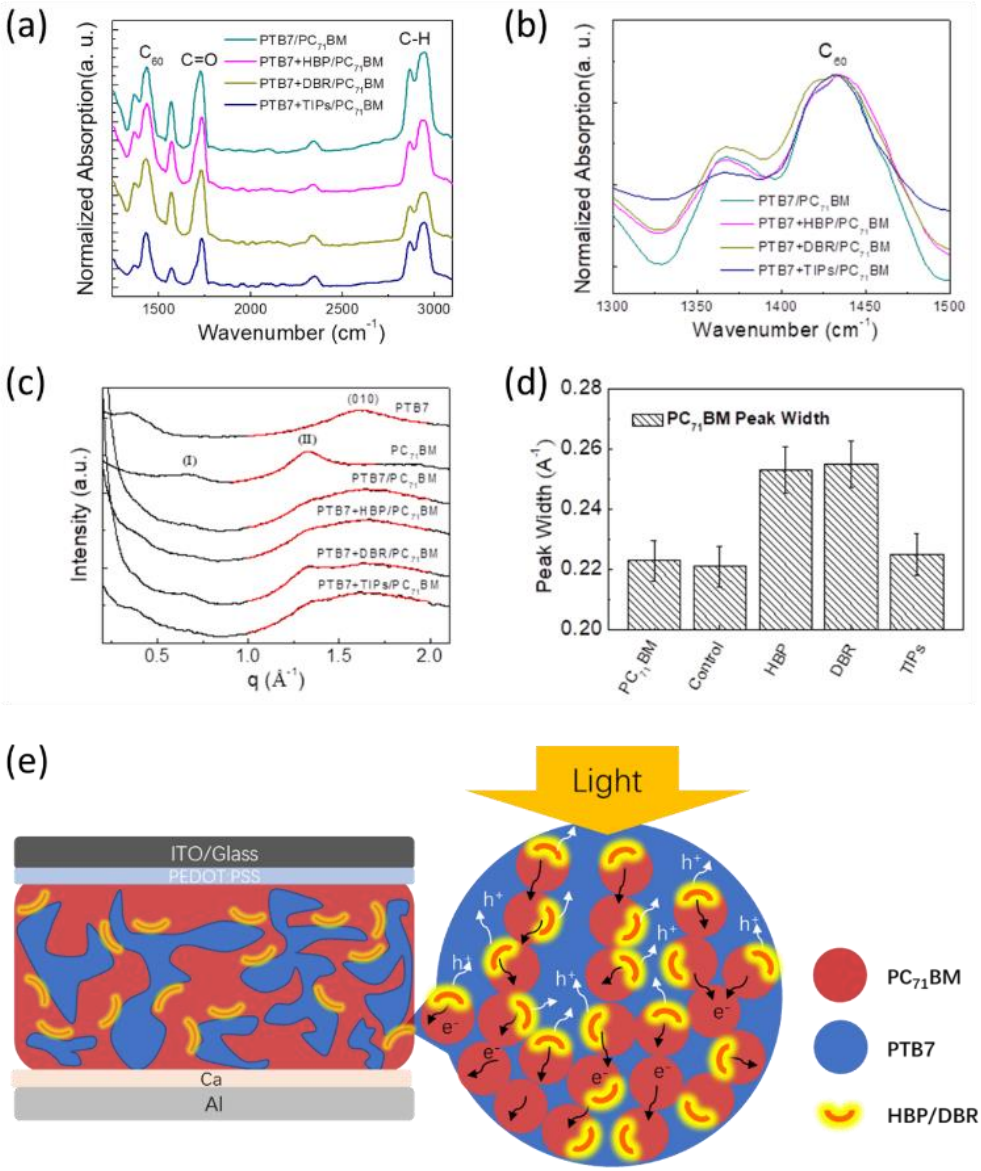


**Figure 7.** (a) The normalized FTIR absorption spectrum of blend active layer films based on PTB7/$PC_{71}BM$ with different additives, (b) The enlarged FTIR absorption spectrum of (a) with wavenumber ranging from 1300 to 1500 $cm^{-1}$. (c) GIXD out-of-plane diffraction patterns (black curves) of the organic blend films and the fitting of the peaks (red curves) with Lorentz functions. (d) The widths of the diffraction peaks at q=1.32 $Å^{-1}$ for $PC_{71}BM$ component in organic films with different additives, which are extracted from the fitting of the peaks. (e) Illustration of the mechanism for the effect of curved additives (HBP/DBR) on the charge transfer and transport in the blend active layer of an OPV.

ARTICLE

**Supplementary information**
Supplementary information

## 4. Conclusions

In summary, highly efficient OPVs are successfully fabricated by introducing high-mobility curved p-type organic semiconductors, HBP and DBR, in the active layers as additives. We demonstrate that HBP can increase the PCE of PTB7/$PC_{71}$BM-based OPVs from 7.80% to 9.54% with a relative enhancement of 22.3% by adding 2.5 wt.% HBP relative to PTB7 in the blend film. For PBDTTT-EFT/$PC_{71}$BM OPVs, the best performance is obtained by incorporating 2.5 wt.% DBR in the active layer. The average PCEs of the OPVs are improved from 9.09% to 10.43% with a relative enhancement of 14.7%. Moreover, the efficiency of the PBDTTT-EFT+DBR/$PC_{71}$BM-based devices could be further improved to 11.42% by adding Au@Ag NCs in the PEDOT:PSS layer due to a plasmonic effect. The significant enhancement of the PCEs by the high-mobility curve molecules can be attributed to the increased hole mobility in the active layer and intimate interactions between the curved molecule and $PC_{71}$BM. In comparison, control experiments by introducing a high-mobility planar molecule additive TIPs-Pentacene only demonstrate a much lower enhancement of the device efficiency, indicating that the molecular structure of the additive is critical to its effect. Therefore, we conclude that the interactions between the additive and donor/acceptor in OPVs play a key role on the photovoltaic performance of OPVs.

## Conflicts of interest

There are no conflicts to declare.

## Acknowledgements

This work is financially supported by the Research Grants Council (RGC) of Hong Kong, China (project number: C4030-14G) and the Hong Kong Polytechnic University (project number: 1-ZVGK and 1-ZVK1).

## Notes and references

1 J. You, L. Dou, K. Yoshimura, T. Kato, K. Ohya, T. Moriarty, K. Emery, C.-C. Chen, J. Gao, G. Li, Y. Yang, *Nat. Commun.,* 2013, 4, 1446.
2 Z. Liu, J. Li, Z.-H. Sun, G. Tai, S.-P. Lau, F. Yan, *ACS Nano,* 2011, 6, 810.
3 G. Li, R. Zhu, Y. Yang, *Nat. Photon.,* 2012, 6, 153.
4 Z. Liu, J. Li, F. Yan, *Adv. Mater.,* 2013, 25, 4296.
5 Z. Liu, P. You, S. Liu, F. Yan, *ACS Nano,* 2015, 9, 12026.
6 L. Dou, J. You, Z. Hong, Z. Xu, G. Li, R. A. Street, Y. Yang, *Adv. Mater.*, 2013, 25, 6642.
7 H. Zhang, H. Yao, J. Hou, J. Zhu, J. Zhang, W. Li, R. Yu, B. Gao, S. Zhang, J. Hou, *Adv. Mater.,* 2018, 30, 1800613.
8 X. Xu, K. Fukuda, A. Karki, S. Park, H. Kimura, H. Jinno, N. Watanabe, S. Yamamoto, S. Shimomura, D. Kitazawa, T. Yokota, S. Umezu, T.-Q. Nguyen, T. Someya, *Proc. Natl. Acad. Sci.*, 2018, 115, 4589.
9 J. Yuan, Y. Zhang, L. Zhou, G. Zhang, H.-L. Yip, T.-K. Lau, X. Lu, C. Zhu, H. Peng, P.A. Johnson, M. Leclerc, Y. Cao, J. Ulanski, Y. Li, Y. Zou, *Joule*, 2019, doi.org/10.1016/j.joule.2019.01.004.
10 H. Ling, S. Liu, Z. Zheng, F. Yan, *Small Methods*, 2018, 1800070.
11 T. Liu, L. Huo, S. Chandrabose, K. Chen, G. Han, F. Qi, X. Meng, D. Xie, W. Ma, Y. Yi, J. M. Hodgkiss, F. Liu, J. Wang, C. Yang, Y. Sun, *Adv. Mater*., 2018, 30, 1707353.
12 S. M. Lee, K. H. Park, S. Jung, H. Park, C. Yang, *Nat. Commun.,* 2018, 9, 1867.
13 J. Wei, G. Ji, C. Zhang, L. Yan, Q. Luo, C. Wang, Q. Chen, J. Yang, L. Chen, C.-Q. Ma, *ACS Nano*, 2018, 12, 5518.
14 P. Cheng, R. Wang, J. Zhu, W. Huang, S.-Y. Chang, L. Meng, P. Sun, H.-W. Cheng, M. Qin, C. Zhu, X. Zhan, Y. Yang, *Adv. Mater.,* 2018, 30, 1705243.
15 D. Li, Z. Xiao, S. Wang, X. Geng, S. Yang, J. Fang, H. Yang, L. Ding, *Adv. Energy Mater.*, 2018, 8, 1800397.
16 S. Liu, S. Lin, P. You, C. Surya, Daniel Lau, F. Yan, *Angew. Chem. Int. Ed.,* 2017, 56, 13717.
17 S. Liu, Y. Hou, W. Xie, S. Schlücker, F. Yan, D. Y. Lei, *Small*, 2018, 14, 1800870.
18 S. Lin, S. Liu, Z. Yang, Y. Li, T. W. Ng, Z. Xu, Q. Bao, J. Hao, C.-S. Lee, C. Surya, F. Yan, S. P. Lau, *Adv. Funct. Mater*., 2016, 26, 864.
19 Z. Liu, S. P. Lau, F. Yan, *Chem. Soc. Rev.*, 2015, 44, 5638.
20 Y. Liu, J. Zhao, Z. Li, C. Mu, W. Ma, H. Hu, K. Jiang, H. Lin, H. Ade, H. Yan, *Nat. Commun*., 2014, 5, 5293.
21 H. Choi, S.-J.Ko, Y. Choi, P. Joo, T. Kim, B. R. Lee, J.-W. Jung, H. J. Choi, M. Cha, J.-R. Jeong, I.-W.Hwang, M. H. Song, B.-S. Kim, J. Y. Kim, *Nat. Photon.,* 2013, 7, 732.
22 S. Liu, R. Jiang, P. You, X. Zhu, J. Wang, F. Yan, *Energ. Environ. Sci.*, 2016, 9, 898.
23 T. Ameri, P. Khoram, J. Min, C. J. Brabec, *Adv. Mater*., 2013, 25, 4245.
24 L. Lu, M. A. Kelly, W. You, L. Yu, *Nat. Photon.*, 2015, 9, 491.
25 L. Lu, T. Zheng, Q. Wu, A. M. Schneider, D. Zhao, L. Yu, *Chem. Rev.,* 2015, 115, 12666.
26 N. Gasparini, M. Salvador, S. Fladischer, A. Katsouras, A. Avgeropoulos, E. Spiecker, C. L. Chochos, C. J. Brabec, T. Ameri, *Adv. Energy Mater*., 2015, 5, 1501527.
27 P. P. Khlyabich, A. E. Rudenko, B. C. Thompson, Y.-L. Loo, *Adv. Funct. Mater., 2015,* 25, 5557.
28 P. Cheng, Y. Li, X. Zhan, *Energ. Environ. Sci.,* 2014, 7, 2005.
29 L. Lu, T. Xu, W. Chen, E. S. Landry, L. Yu, *Nat. Photon.,* 2014, 8, 716.
30 S. Liu, P. You, J. Li, J. Li, C.-S. Lee, B. S. Ong, C. Surya, F. Yan, *Energ. Environ. Sci.*, 2015, 8, 1463.

31 J. Li, Y. Zhao, H. S. Tan, Y. Guo, C.-A. Di, G. Yu, Y. Liu, M. Lin, S. H. Lim, Y. Zhou, H. Su, B. S. Ong, *Sci. Rep*., 2012, 2, 754.
32 H.-R. Tseng, H. Phan, C. Luo, M. Wang, L. A. Perez, S. N. Patel, L. Ying, E. J. Kramer, T.-Q. Nguyen, G. C. Bazan, A. J. Heeger, *Adv. Mater.,* 2014, 26, 2993.
33 J. Kang, N. Shin, D. Y. Jang, V. M. Prabhu, D. Y. Yoon, *J. Am. Chem. Soc.,* 2008, 130, 12273.
34 B. Park, H. G. Jeon, J. Choi, Y. K. Kim, J. Lim, J. Jung, S. Y. Cho, C. Lee, *J. Mater. Chem.*, 2012, 22, 5641.
35 J. J. Kim, H. M. Lee, J. W. Park, S. O. Cho, *J. Mater. Chem. C*, 2015, 3, 2650.
36 Y. Yuan, G. Giri, A. L. Ayzner, A. P. Zoombelt, S. C. B. Mannsfeld, J. Chen, D. Nordlund, M. F. Toney, J. Huang, Z. Bao, *Nat. Commun.,* 2014, 5, 3005.
37 L. Shan, D. Liu, H. Li, X. Xu, B. Shan, J.-B. Xu, Q. Miao, *Adv. Mater.*, 2015, 27, 3418.
38 X. Gu, X. Xu, H. Li, Z. Liu, Q. Miao, *J. Am. Chem. Soc.,* 2015, 137, 16203.
39 Z. Liang, Q. Tang, J. Xu, Q. Miao, *Adv. Mater., 2011,* 23, 1535.
40 J. Luo, X. Xu, R. Mao, Q. Miao, *J. Am. Chem. Soc., 2012,* 134, 13796.
41 Q. Tai, J. Li, Z. Liu, Z. Sun, X. Zhao, F. Yan, *J. Mater. Chem.*, 2011, 21, 6848.
42 W. Zhao, S. Li, H. Yao, S. Zhang, Y. Zhang, B. Yang, J. Hou, *J. Am. Chem. Soc*., 2017, 139, 7148.
43 R. Jiang, H. Chen, L. Shao, Q. Li, J. Wang, *Adv. Mater.,* 2012, 24, OP200.
44 S. Dai, T. Li, W. Wang, Y. Xiao, T.-K. Lau, Z. Li, K. Liu, X. Lu, X. Zhan, *Adv. Mater.,* 2018, 30, 1706571.
45 S. H. Yoo, J. M. Kum, S. O. Cho, *Nanoscale Res. Lett.,* 2011, 6, 545.
46 C. Deibel, T. Strobel, V. Dyakonov, *Adv. Mater.*, 2010, 22, 4097.
47 F. Machui, S. Rathgeber, N. Li, T. Ameri and C. J. Brabec, *J. Mater. Chem.,* 2012, 22, 15570.